Journal of the Ceramic Society of Japan 117 [4] 466-469 2009 **Paper**

Thermoelectricity of $CaIrO_3$ ceramics prepared by spark plasma sintering

Nittaya KEAWPRAK,† Rong TU and Takashi GOTO

Institute for Materials Research, Tohoku University, Sendai 980−8577

Polycrystalline bulk $CaIrO_3$ as a main phase with minor phases of IrO_2 and/or Ca_2IrO_4 was prepared by spark plasma sintering (SPS) at 1273 K. Metastable $CaIrO_3$ with a perovskite-type structure (pv-$CaIrO_3$) formed by heat-treatment at 1273 K for 43.2 ks and transformed into a post-perovskite structure (ppv-$CaIrO_3$) by heat-treatment at 1273 K for 259.2 ks. The electrical conductivity (σ) of the pv-$CaIrO_3$ specimen decreased from 1.74×10^4 to 1.45×10^4 Sm^{-1}, while the σ of the ppv-$CaIrO_3$ specimen increased from 5.0×10^1 to 9.8×10^2 Sm^{-1} with increasing temperature from 298 to 1023 K. The Seebeck coefficient (S) of the pv-$CaIrO_3$ specimen was around −44 μVK^{-1} at room temperature and increase to the highest value of 40 μVK^{-1} at 1023 K. The S of the ppv-$CaIrO_3$ specimen decreased with increasing temperature and had an almost constant value of about 60 μVK^{-1} above 600 K. The thermal conductivity (κ) of the ppv-$CaIrO_3$ specimen decreased from 2.7 to 1.2 $Wm^{-1}K^{-1}$ and that of the pv-$CaIrO_3$ specimen decreased from 1.5 to 1.2 $Wm^{-1}K^{-1}$ with increasing temperature from 298 to 1023 K. The highest dimensionless figure of merit values (ZT) of the pv-$CaIrO_3$ and the ppv-$CaIrO_3$ specimens were 0.02 and 0.003 at 1023 K, respectively.

Key-words : Thermoelectric materials, Calcium Iridium oxide, Spark plasma sintering

[Received December 18, 2008; Accepted February 19, 2009]

1. Introduction

IrO_2 has been applied as electrodes and electrical conducting pastes because of its excellent electrical conductivity. However, IrO_2 evaporates by forming volatile IrO_3 in an oxidation atmosphere at high temperatures. Alkaline earth iridium oxides such as $CaIrO_3$ and $SrIrO_3$ have been proposed to solve this problem. McDaniel et al. have reported two polymorphisms of perovskite-type and post-perovskite-type $CaIrO_3$. The perovskite $CaIrO_3$ (pv-$CaIrO_3$) is a metastable phase which can be prepared by solid state reaction in air[1] between 1173 and 1273 K, accompanying with a stable phase of post-perovskite $CaIrO_3$ (ppv-$CaIrO_3$). The space group of ppv-$CaIrO_3$ is *Cmcm* and its lattice parameters are a = 0.31445, b = 0.98656 and c = 0.72986 nm. pv-$CaIrO_3$ belongs to a space group of *Pbnm* and its lattice parameters are a = 0.53478, b = 0.55935 and c = 0.76757 nm.[2] The compressibility of ppv-$CaIrO_3$ is higher than that of pv-$CaIrO_3$.[3] The thermodynamic properties of $CaIrO_3$ have been studied, particularly to investigate the transition from the perovskite to the post-perovskite-type structures.[2] The ppv-$CaIrO_3$ in a single phase has been hardly synthesized in an ambient atmosphere and usually coexisted with of Ca_2IrO_4. Recently, Niwa et al. synthesized the two types of $CaIrO_3$ in a single phase under a high pressure from 1 to 5 GPa at 1450–1550 K.[4] Sarkozy et al.[5] have prepared the pv-$CaIrO_3$ by a combined process of solid state reaction and hydroxide precipitation. The properties of pv-and ppv-$CaIrO_3$ have not been well studied. It has been merely reported that the pv-$CaIrO_3$ is a metallic conductor with less than 1 Ω at room temperature.

Recently, our research group has reported moderately high thermoelectric properties of $CaRuO_3$. The pv- and ppv-$CaIrO_3$ could be also a candidate thermoelectric material due to the similarity between $CaRuO_3$ and $CaIrO_3$. In the present study, we have prepared the pv- and ppv-$CaIrO_3$ specimens by spark plasma sintering (SPS) and investigated their electrical conductivity (σ), thermal conductivity (κ), Seebeck coefficient (S) and dimensionless figure of merit (ZT).

† Corresponding author: N. Keawprak; E-mail: nittaya@imr.tohoku.ac.jp

2. Experimental procedure

The $CaCO_3$ (99.5%) and Ir (99.9904%) powders were mixed with a molar ratio Ir:Ca = 1:1 and pressed into pellets and then reacted at 1173–1323 K for 43.2–259.2 ks in air. The calcined pellets were crushed and compacted again by SPS at 1273 K for 0.18 ks in a vacuum at 80 MPa. The compacted body was cut to $2 \times 2 \times 10$ mm for the measurements of electrical conductivity by a d.c. 4-probe method and Seebeck coefficient by a thermoelectric power (ΔE)-temperature difference (ΔT) method. A disk-shaped specimen 10 mm in diameter and 1 mm in thickness was employed to measure thermal conductivity by a laser flash method (ULVAC TC–7000). All measurements were conducted from room temperature (RT) to 1023 K. The crystal phase was examined by X-ray diffraction (XRD, Rigaku Geigerflex). The composition was examined by electron probe micro-analysis (EPMA). The microstructure was observed by scanning electron microscopy (SEM). The density (d) was determined by an Archimedes method.

3. Results and discussion

Figure 1 presents XRD patterns of the calcined powders at various temperatures for 7.2 ks. At 1173 K, a mixture of pv-$CaIrO_3$, Ca_2IrO_4 and a small amount of IrO_2 was formed (Fig. 1(a)). The ppv-$CaIrO_3$ phase appeared at 1223 K (Fig. 1(b). The content of ppv-$CaIrO_3$ increased and that of Ca_2IrO_4 decreased with increasing temperature to 1273 K (Figs. 1(b) and (c)). Ca_2IrO_4 became to be a main phase at 1323 K with a small

amount of IrO_2 and $CaIrO_3$ (Fig. 1(d)).

Figure 2 shows XRD patterns of the calcined powders at 1273 K for various calcining times. In the early stage of the calcination by 43.2 ks, pv-$CaIrO_3$ with a small amount of ppv-$CaIrO_3$ and Ca_2IrO_4 was identified (Fig. 2(a)). pv-$CaIrO_3$ was obtained as a main phase at 1273 K for 43.2 ks. The content of pv-$CaIrO_3$ decreased with increasing calcining time and disappeared after 259.2 ks (Fig. 2(d)), whereas ppv-$CaIrO_3$ became to a main phase. This implied that the pv-$CaIrO_3$ was transformed into the stable phase by heat-treatment at 1273 K for 259.2 ks. A small amount of Ca_2IrO_4 co-existed, but decreased with increasing calcining time. The lattice parameters of the pv-$CaIrO_3$ were a = 0.5346, b = 0.7675 and c = 0.5586 nm and those of the ppv-$CaIrO_3$ were a = 0.3148, b = 0.9866 and c = 0.7300 nm, showing almost the same values as those reported by McDaniel.[1] ppv-$CaIrO_3$ almost in a single phase was obtained at 1273 K for 259.2 ks.

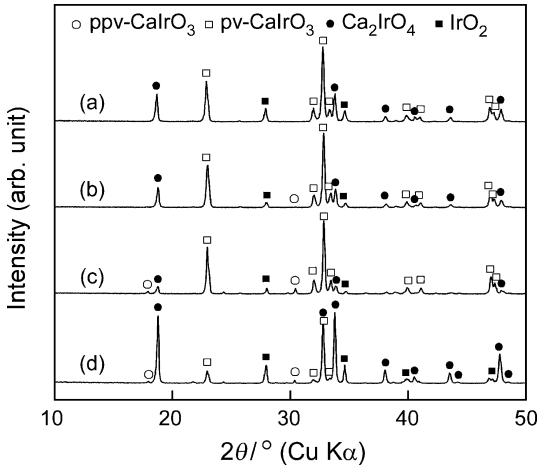

Fig. 1. XRD patterns of powders calcined at 1173(a), 1223(b), 1273(c) and 1323 K(d) for 7.2 ks.

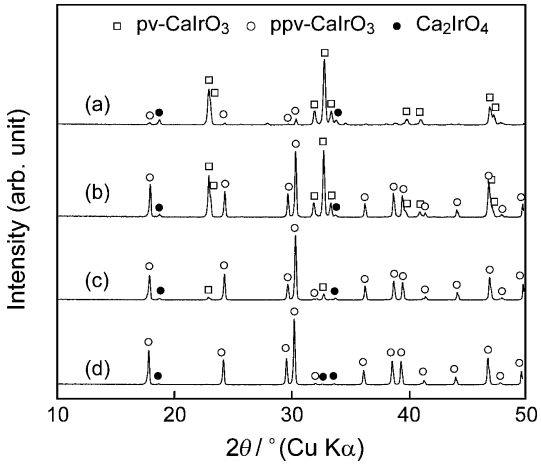

Fig. 2. XRD patterns of powders calcined at 1273 K for 43.2(a), 129.6(b), 216.0(c) and 259.2 ks(d).

The powders of pv-$CaIrO_3$ and ppv-$CaIrO_3$ as main phases were compacted by SPS to make bulk specimens to measurement thermoelectric properties. **Figure 3** shows the XRD patterns of ppv-$CaIrO_3$ and pv-$CaIrO_3$ bulk specimens compacted by SPS at 1273 K for 180 s. The crystal phases were almost the same as that of the starting calcined powders. However, a small amount of Ir metal phase was identified. This might have been resulted from the decomposition in a vacuum and from the slight reduction by the surrounding graphite die. The Ir metal phase still existed in an Ar gas atmosphere, while it disappeared in air after heat-treatment at 1273 K.

Figure 4 shows the fracture microstructure of the compacted bulk bodies. The ppv-$CaIrO_3$ specimen consisted of rod-like grains of about 10 μm in length (Fig. 4(a)), while the pv-$CaIrO_3$ specimen contained rounded grains of 5 μm in diameter (Fig. 4(b)). The small grains of 1 μm in diameter and the elongated grains in Fig. 4(b) were identified as Ca_2IrO_4 and ppv-$CaIrO_3$, respectively. The relative densities of pv- and ppv-$CaIrO_3$ speci-

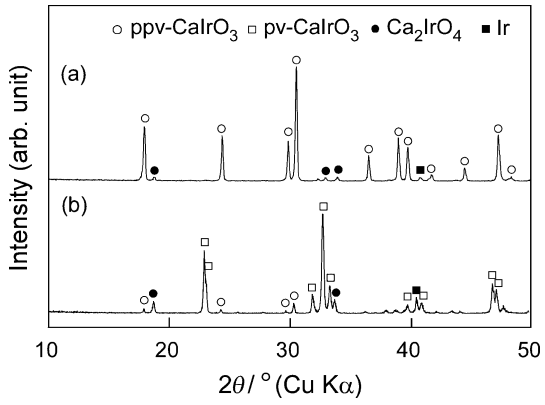

Fig. 3. Powder XRD patterns of ppv-$CaIrO_3$ (a) and pv-$CaIrO_3$ (b) specimen sintered at 1273 K.

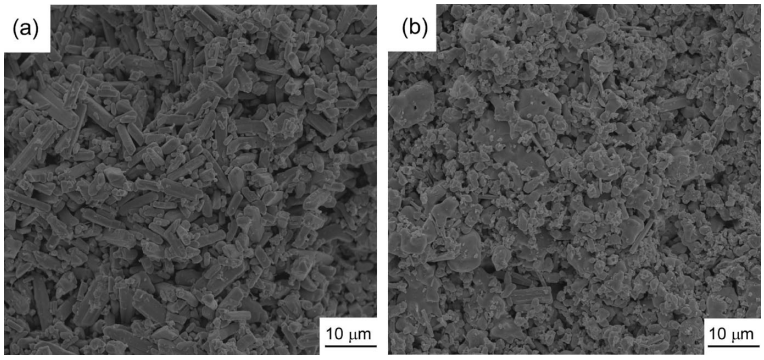

Fig. 4. SEM images of the fracture cross section of ppv-$CaIrO_3$ (a) and pv-$CaIrO_3$ specimens (b).

mens were 62 and 66%, respectively. Although the SPS is commonly able to prepare dense bodies, highly dense $CaIrO_3$ bodies were not obtained mainly because of the low sintering temperature (1273 K) to avoid the decomposition and of signification grain growth probably through a vapor phase transport. At higher sintering temperature above 1273 K, a large amount of Ir metal phase appeared in which the compacted bulk bodies become denser.

Figure 5 presents the temperature dependence of electrical conductivity (σ) for the pv- and ppv-$CaIrO_3$ specimens. The σ of the pv-$CaIrO_3$ specimen decreased with increasing temperature from RT to 1023 K, showing a metallic conduction. On the other hand, the σ of the ppv-$CaIrO_3$ specimen increased with increasing temperature, exhibiting a semiconducting conduction, whose σ was much lower than that of pv-$CaIrO_3$ specimen. The ppv-$CaIrO_3$ specimen might have different conduction mechanism depending on temperature. The activation energy at high temperature regions was 0.15 eV.

Figure 6 shows the temperature dependence of the Seebeck coefficient (S) for the pv- and ppv-$CaIrO_3$ specimens. The S of the pv-$CaIrO_3$ specimen showed negative values around −44 μVK^{-1} at RT and increased to positive values above 500 K with the highest value of 40 μVK^{-1}. The negative S might have been affected by a small amount of secondary phase of Ca_2IrO_4. Our previous study reported that Ca_2IrO_4 had a negative S of –100 to –40 μVK^{-1} from RT to 1023 K.[6] The S of the ppv-$CaIrO_3$ specimen decreased from 550 to 60 μVK^{-1} with increasing temperature from RT to 600 K and then became an almost constant value of around 60 μVK^{-1} above 600 K.

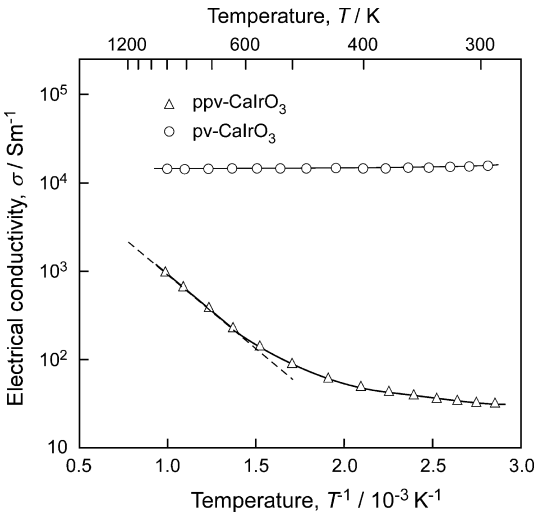

Fig. 5. Temperature dependence of electrical conductivity (σ) for pv-$CaIrO_3$ and ppv-$CaIrO_3$ specimens.

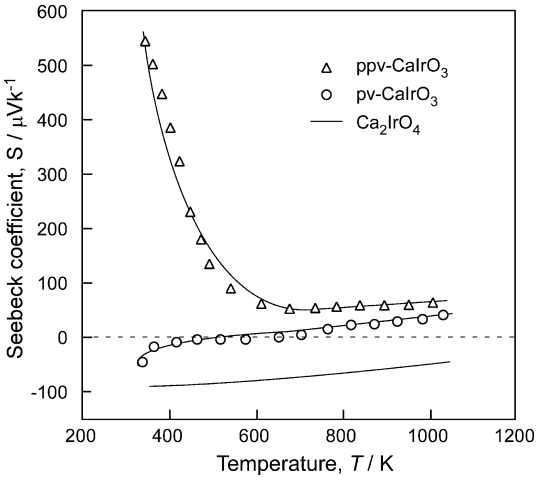

Fig. 6. Temperature dependence of seebeck coefficient (S) measured for pv-$CaIrO_3$ and ppv-$CaIrO_3$ specimens.

Figures 7(a) and (b) depict the crystal structures of pv- and ppv-$CaIrO_3$. In the structure of ppv-$CaIrO_3$, Ir atom centered oxygen octahedra share edges and form two dimensional IrO_3 layers in the a–c plane. Each layer is separated by Ca atoms. The edge-sharing IrO_6 octahedra layers separated by Ca atoms in ppv-$CaIrO_3$ may be related to the non-metallic behavior because of non-overlapping between Ir-5d and O-2p in the b-axis direction. In the orthorhombic perovskite-type structure of pv-$CaIrO_3$, IrO_6 octahedra share all axes and form a three-dimensional network which may cause strong overlap between Ir-5d and O-2p leading metallic conduction similar to the case of $CaRuO_3$.[6]

Figure 8 presents the temperature dependence of thermal conductivity (κ) for the pv- and ppv-$CaIrO_3$ specimens. The κ of the pv-$CaIrO_3$ and ppv-$CaIrO_3$ specimens at RT were 1.5 and 2.5 $Wm^{-1}K^{-1}$, respectively. The κ of both specimens decreased to 1.0 $Wm^{-1}K^{-1}$ with increasing temperature to 700 K and then slightly increased at higher temperatures.

The ZT values of both samples increased with increasing temperature as shown in **Fig. 9**. The highest ZT values of the pv- and ppv-$CaIrO_3$ specimens were 0.018 and 0.003 at 1023 K, respectively. The pv-$CaIrO_3$ specimen showed higher ZT values than those of the ppv-$CaIrO_3$ specimen mainly due to higher σ.

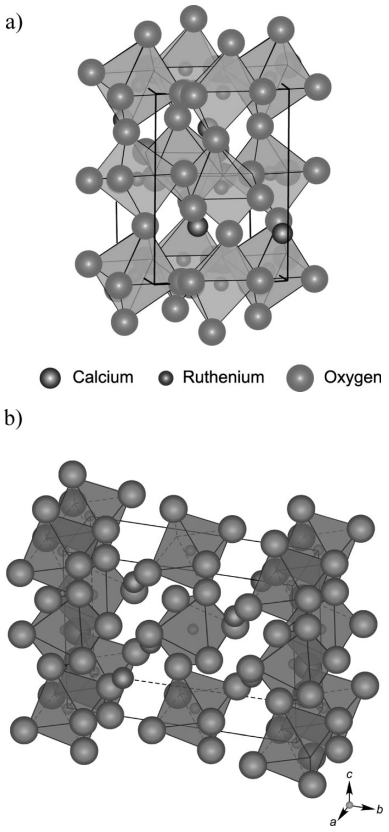

Fig. 7. Crystal structure of pv-$CaIrO_3$ (a) and ppv-$CaIrO_3$ (b).

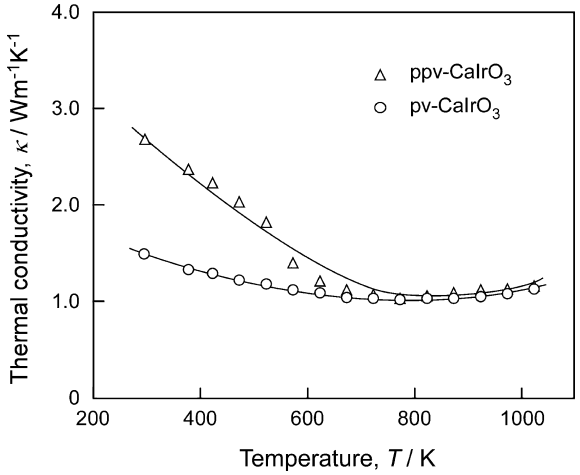

Fig. 8. Temperature dependence of thermal conductivity (κ) for pv-$CaIrO_3$ and ppv-$CaIrO_3$ specimens.

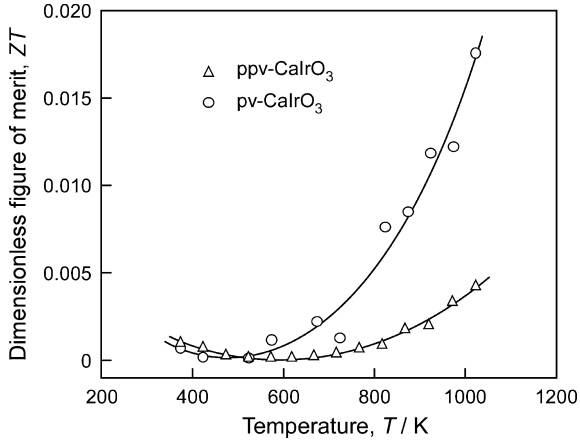

Fig. 9. Temperature dependence of dimensionless figure of merit (ZT) for pv-$CaIrO_3$ and ppv-$CaIrO_3$ specimens.

4. Conclusions

Metastable perovskite (pv) and post-perovskite (ppv) $CaIrO_3$ bulk specimens were prepared by spark plasma sintering (SPS) using $CaCO_3$ and Ir as starting powders. The σ of the pv-$CaIrO_3$ specimen showed a metallic conduction whereas that of the ppv-$CaIrO_3$ specimen showed a semiconducting behavior. The S of the pv-$CaIrO_3$ specimen increased from –44 to 40 μVK^{-1} with increasing temperature from RT to 1023 K, while that of the ppv-$CaIrO_3$ phase decreased from 550 to 60 μVK^{-1} with increasing temperature. The κ of the ppv-$CaIrO_3$ specimen decreased from 2.7 to 1.0 $Wm^{-1}K^{-1}$ and that of the ppv-$CaIrO_3$ specimen slightly decreased from 1.5 to 1.0 $Wm^{-1}K^{-1}$ from RT to 600 K. The highest ZT values of the pv- and ppv-$CaIrO_3$ specimens were 0.018 and 0.003 at 1023 K.

Acknowledgement The authors are grateful to global COE program, JSPS Asian CORE program, Furuya Metal Co., Ltd. and Lonmin Plc. for financial support.

References

1) C. L. McDaniel and S. J. Schneider, *J. Solid State Chem.*, **4**, 275 (1972).
2) H. Kojitani, A. Furukawa and M. Akaogi, *Am. Mineral.*, **92**, 229 (2007).
3) T. B. Ballaran, R. G. Tronnes and D. J. Frost, *Am. Mineral.*, **92**, 1760 (2007).
4) K. Niwa, T. Tagi, K. Ohgushi, S. Merkel, N. Miyajima and T. Kikegawa, *Phys. Chem. Minerals*, **34**, 679 (2007).
5) R. F. Sarkozy, C. W. Moeller and B. L. Chamberland, *J. Solid State Chem.*, **9**, 242 (1974).
6) N. Keawprak, R. Tu and T. Goto, *Mat. Trans.*, **48**, 1529 (2007).